Acetylcholine Receptor Gating: Movement in the α-Subunit Extracellular Domain

Prasad Purohit and Anthony Auerbach

Department of Physiology and Biophysics, State University of New York at Buffalo, Buffalo, NY 14214

Acetylcholine receptor channel gating is a brownian conformational cascade in which nanometer-sized domains ("Φ blocks") move in staggering sequence to link an affinity change at the transmitter binding sites with a conductance change in the pore. In the α-subunit, the first Φ-block to move during channel opening is comprised of residues near the transmitter binding site and the second is comprised of residues near the base of the extracellular domain. We used the rate constants estimated from single-channel currents to infer the gating dynamics of Y127 and K145, in the inner and outer sheet of the β-core of the α-subunit. Y127 is at the boundary between the first and second Φ blocks, at a subunit interface. αY127 mutations cause large changes in the gating equilibrium constant and with a characteristic Φ-value (Φ = 0.77) that places this residue in the second Φ-block. We also examined the effect on gating of mutations in neighboring residues δI43 (Φ = 0.86), εN39 (complex kinetics), αI49 (no effect) and in residues that are homologous to αY127 on the ε, β, and δ subunits (no effect). The extent to which αY127 gating motions are coupled to its neighbors was estimated by measuring the kinetic and equilibrium constants of constructs having mutations in αY127 (in both α subunits) plus residues αD97 or δI43. The magnitude of the coupling between αD97 and αY127 depended on the αY127 side chain and was small for both H (0.53 kcal/mol) and C (−0.37 kcal/mol) substitutions. The coupling across the single α–δ subunit boundary was larger (0.84 kcal/mol). The Φ-value for K145 (0.96) indicates that its gating motion is correlated temporally with the motions of residues in the first Φ-block and is not synchronous with those of αY127. This suggests that the inner and outer sheets of the α-subunit β-core do not rotate as a rigid body.

The Journal of General Physiology

INTRODUCTION

The diliganded gating isomerization of the acetylcholine receptor (AChR), between C(losed) and O(pen) structures, is a conformational "wave" that links a change in affinity for ligands at the transmitter binding sites with a change in the ionic conductance of the pore. In the α-subunit, the first group of amino acids to undergo a C→O structural change is near the transmitter binding sites (Akk et al., 1996; Corringer et al., 2000; Chakrapani et al., 2003). Homologous residues in the ACh binding protein (AChBP) have been shown to change conformation as a result of agonist binding (Brejc, 2001; Celie et al., 2004; Hansen et al., 2005). The second group of residues to move in gating is near the base of the extracellular domain (ECD), in loops 2 and 7 (the "cys-loop") (Chakrapani et al., 2004). These ECD movements subsequently propagate into the transmembrane domain (TMD), toward an equatorial "gate" in M2 that regulates the conductance of the pore.

The relative timing of a residue's gating motion can be inferred from the rate constants of the diliganded C↔O gating reaction (Auerbach, 2007). The slope Φ of a log–log plot of the opening rate constant vs. the equilibrium constant for a series of mutations of a single residue is thought to give the relative time in the channel-opening process that the mutated residue converts from C to its O structure. In the extracellular region of the α-subunit, Φ values decrease from the transmitter binding site (Φ = 0.93), to the cys-loop and loop 2 (Φ = 0.78), to the M2–M3 linker (Φ = 0.64).

Currently, there is a model for the structure of closed-unliganded *Torpedo* AChRs, ∼4-Å resolution (Unwin, 2005), in which the β cores of the ECD of the two α subunits are rotated with respect to those in the three non–α subunits. This observation led to the proposal that during diliganded C→O gating (as opposed to agonist binding) there is a symmetry-restoring rotation of the inner β-sheet of the α-subunit ECD.

Here we report the results of mutations on gating of two α-subunit residues that are near the top of the inner (strands 1, 2, 3, 5, 6, and 8) and outer (strands 4, 7, 9, and 10) β sheets of the α-subunit, Y127 (on β-strand 6), and K145 (on β-strand 7). αY127 lies at a boundary between the first two Φ blocks, with its atoms <4 Å from residues in both αD97 in loop A (Φ = 0.93) in the *Torpedo* AChR structure (Unwin, 2005). However, αY127 and αD97 are ∼9 Å apart in the mouse α-subunit ECD fragment

Correspondence to Anthony Auerbach: auerbach@buffalo.edu

Abbreviations used in this paper: AChBP, ACh binding protein; AChR, acetylcholine receptor; ECD, extracellular domain; REFER, rate-equilibrium free energy relationship; TMD, transmembrane domain; wt, wild type.

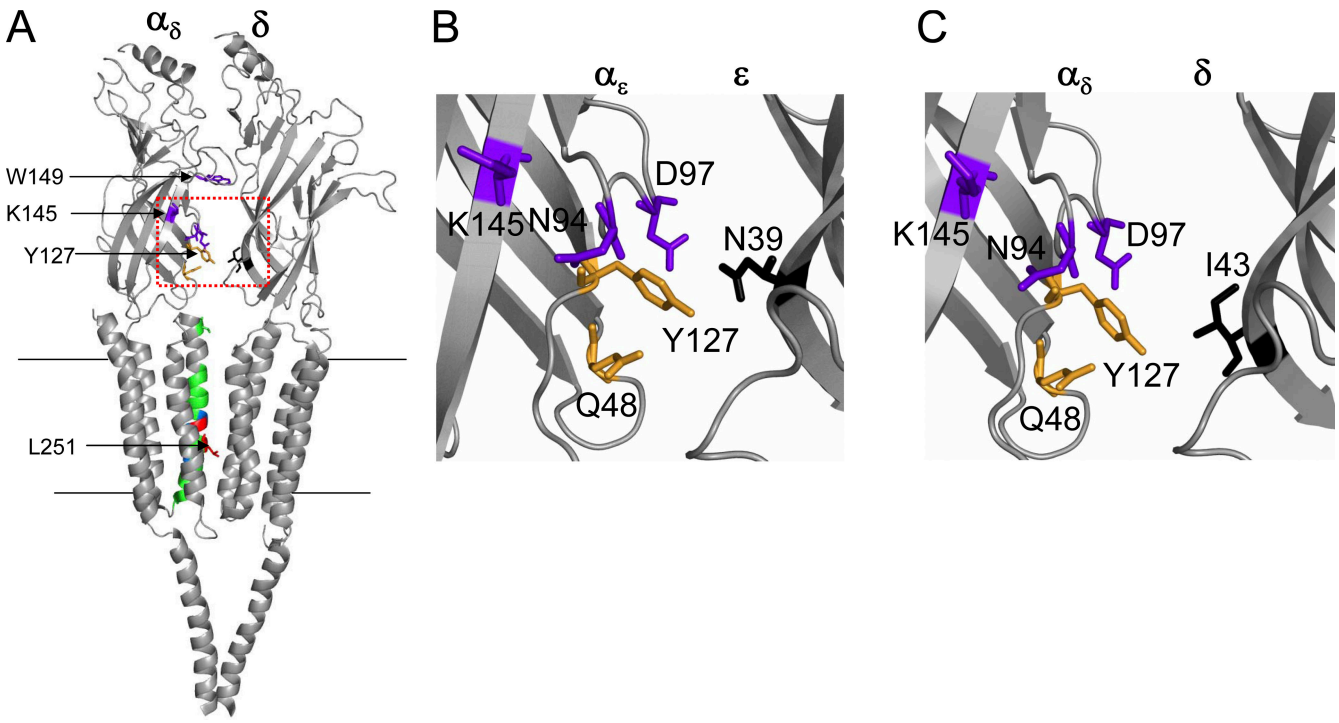

Figure 1. Location of αY127 in *Torpedo* AChRs. (A) A Cartoon of the $\alpha_\varepsilon/\delta$ subunits viewed from the exterior of the AChR. Only the α_ε (left) and ε subunits are shown; the horizontal lines mark, approximately, the membrane. In α_δ the three Φ blocks that link the transmitter binding site with the gate are color coded as purple (Φ = 0.93, W149, K145), orange (Φ = 0.78, Y127), green (Φ = 0.65, S269), and red (Φ = 0.31, L251). (B and C) Expansion of boxed region in A. αK145 (purple) is on β-strand 7 and αY127 (orange) at the $\alpha_\varepsilon/\varepsilon$ (B) and α_δ/δ (C) subunit interface. αY127 is <4 Å from residues αD97 and αN94 in loop A (purple), αQ48 in loop 2 (orange), and εN39/δI43 in β-strand 1 (black). Structures were displayed by using PYMOL (DeLano Scientific).

structure (2qc1.pdb, Dellisanti et al., 2007). αY127 is located at or near the C terminus of β-strand 6, one position from the C128–C142 disulfide bond that defines the cys-loop (loop 7) of the eukaryote pentameric receptor superfamily (Fig. 1). αY127 also is at a subunit interface and faces either the ε (γ in embryonic AChRs) or δ subunit, and for this reason the structure of this residue is poorly resolved in the monomeric ECD fragment (Dellisanti et al., 2007). Mukhtasimova and Sine (2007) found that the mutation αY127T substantially decreases K_{eq}, as do the mutations εN39A and δN41A in nearby residues in these non–α subunits. Moreover, the effects of these perturbations were not independent, which suggests that these positions are coupled energetically and are a link for the intersubunit propagation of the gating conformational cascade.

In both the *Torpedo* AChR and ECD fragment structures, αK145 is <4 Å from two residues whose mutation significantly changes K_{eq}, αD200 (in loop C) and αY93 (in loop A) (Akk et al., 1996; Akk, 2001). Although rate constants for only a few mutations of each of these positions have been measured, the values are consistent with a Φ-value near 1, which places these neighboring amino acids in the first, Φ = 0.93 block. M144, next to K145 in sequence, was measured to have a Φ-value of 0.84 ± 0.05. Mukhtasimova et al. (2005) found that substitution of A, Q, and E side chains at αK145 all reduce K_{eq} substantially and that the effect of αK145E and αD200N mutations are not energetically independent, and proposed that interactions between αK145–αD200 vs. αK145–αY190 (based on structure) stabilize the C vs. O conformation, respectively.

We have extended these studies regarding αY127 and αK145 by more extensive Φ-value analysis, and have related the results to the ECD rotation hypothesis for gating. First, we measured rate constants from single-channel currents and estimated Φ for αY127 (all 20 natural amino acid side chains) and its neighbor in the δ-subunit, I43. Second, we estimated the magnitude of the energetic coupling between αY127 and either δI43 or αD97, in six different constructs. Third, we examined the kinetic behavior of mutations to residues in the ε, δ, and β subunits that are homologous to αY127. Fourth, we measured the diliganded gating rate constants of four mutants of position αK145. The results show that a point side chain substitution at αY127 can change K_{eq} by a factor of ∼290,000, that αY127 is a member of the second Φ-block, that the coupling between αY127 and αD97 or δI43 is measurable but small (<1 kcal/mol). Regarding αK145, mutations alter the channel opening rate (relative to the change in K_{eq}) to a greater extent than for αY127, which suggests that

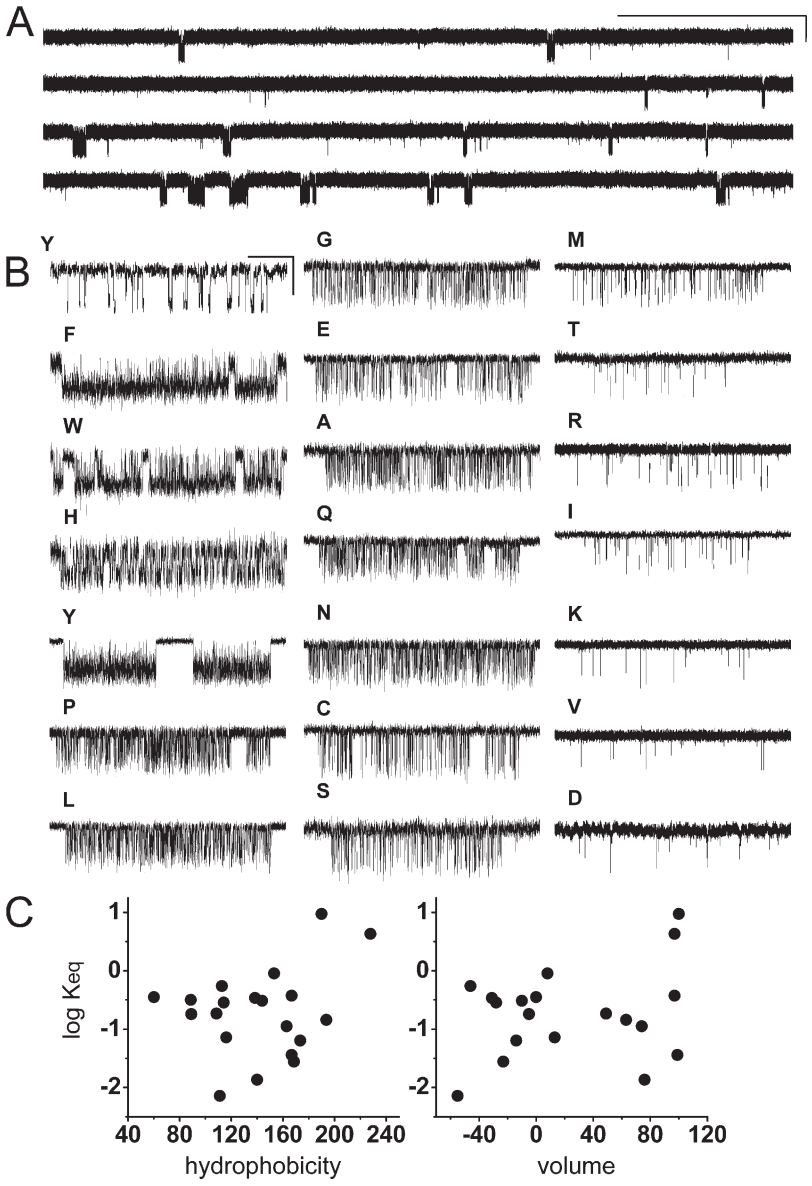

Figure 2. Example single-channel traces for 19 different side chains at αY127. (A) Continuous, low time resolution view of Y127F single-channel currents elicited by 20 mM choline (low pass filtered at 2 kHz for clarity; calibrations: 4 s, 2 pA). In the continued presence of such a high concentration of agonist, openings occur in clusters (open is down) separated by long nonconducting sojourns in "desensitized" states. Each cluster reflects C↔O gating of a single AChR. (B) Three gain-of-function constructs (F, W, and H) were activated by 20 mM choline and the current elicited for all other mutants were by 500 μM ACh. Example cluster for WT is shown for both the agonists. Calibration bars: (horizontal = 100 ms for choline and ACh, vertical scale bar = 2 pA, choline and 6 pA, ACh). (B) There was no apparent correlation of the side chain hydrophobicity or volume with the change in the diliganded gating equilibrium constant (K_{eq}). The r values were 0.26 (hydrophobicity) and 0.28 (volume).

these two residues do not move synchronously in the gating reaction.

MATERIALS AND METHODS

For the details of mutagenesis, expression, electrophysiology, rate constant determination, and Φ-value analysis, see Jha et al. on page 547 of this issue. In brief, mouse AChR subunits were transiently expressed in HEK 293 cells and recordings were from cell-attached patches (22°C, ∼−100 mV membrane potential). Agonist was added to the pipette solution (500 μM ACh, 5 mM carbamylcholine, or 20 mM choline). Currents were analyzed with QUB software (www.qub.buffalo.edu). Opening and closing rate constants were estimated from interval durations by using a maximum-interval likelihood algorithm (Qin et al., 1997) after imposing a dead time of 25 μs. Φ was estimated as the slope of the rate-equilibrium free energy relationship (REFER), which is a plot of log k_o vs. log K_{eq}. Each point in the plot represents the mean of at least three different patches.

RESULTS

Mutations of αY127 and its Homologues

In vertebrate α_1 subunits, position 127 is always a Y but in non–α_1 subunits it is never a Y (but is, rather, S, A, T, or V). A tyrosine at position 127 is a specific marker for the vertebrate neuromuscular α_1-subunit. The location of Y127 in the *Torpedo* AChR structure is shown in Fig. 1.

Fig. 2 and Table I show the results of single-channel kinetic analyses of wild-type AChRs plus all 19 natural amino acid substitutions at αY127. 16 of the mutations decreased K_{eq} (D by ∼4,900-fold) while the three aromatic

TABLE I

Kinetic Analyses of AChR Mutants

Construct	Agonist	k_0 (s^{-1})	k_c^{obs} (s^{-1})	k_c^{cor} (s^{-1})	K_{eq} (k_o/k_c^{cor})	Normalized K_{eq} (mut/wt)	*n*
wt	Cho[a]	120	–	2583	0.046	1	–
wt	ACh[b]	48000	–	1700	28.2	1	–
wt	CCh	7721	–	1138	6.8	1	–
Y127F	Cho	2853 (221)	390 (20.3)	1041.3 (107)	2.7 (0.28)	58.7	4
Y127W	Cho	1518 (170)	353 (122)	943 (234)	1.6 (0.4)	34.8	2
Y127H	Cho	520 (68)	577 (86)	1541 (295)	0.33 (0.01)	7.2	4
Y127P	ACh	3008	5498	6872.5	0.43	0.015	1
Y127L	ACh	2351 (217)	6277 (536)	7846 (670)	0.29 (0.05)	0.01	4
Y127G	ACh	2009 (95)	5676 (247)	7095 (309)	0.28 (0.03)	0.01	2
Y127E	ACh	1166 (153)	3411 (306)	4264 (382)	0.27 (0.05)	0.01	4
Y127A	ACh	1726 (97)	5447 (332)	6809 (416)	0.25 (0.03)	0.009	3
Y127Q	ACh	1570 (70)	5126 (104)	6408 (130)	0.24 (0.01)	0.009	5
Y127N	ACh	1574 (36)	5506 (353)	6883 (441)	0.22 (0.01)	0.008	3
Y127C	ACh	862 (119)	4674 (248)	5843 (310)	0.14 (0.03)	0.005	4
Y127S	ACh	1076 (94)	5953 (522)	7442 (653)	0.14 (0.03)	0.005	2
Y127M	ACh	555 (101)	4952 (340)	6190 (425)	0.089 (0.02)	0.003	4
Y127T	ACh	550 (7)	7619 (569)	9524 (711)	0.057 (0.004)	0.002	4
Y127R	ACh	336 (25)	5273 (363)	6591 (454)	0.051 (0.003)	0.0018	3
Y127I	ACh	208 (44)	5763 (533)	7204 (667)	0.028 (0.006)	0.001	2
Y127K	ACh	238 (57)	8556 (585)	10690 (732)	0.022 (0.005)	0.0008	3
Y127V	ACh	112 (4)	8230 (1388)	10288 (1374)	0.010 (0.001)	0.0004	3
Y127D	ACh	29 (12)	3966 (435)	4958 (543)	0.0057 (0.002)	0.0002	3
Y127P	CCh	2956	2386	5843	0.51	0.075	1
Y127A	CCh	603 (38)	2600 (91)	6162 (517)	0.098 (0.01)	0.014	3
Y127E	CCh	175 (21)	1082 (274)	2617 (651)	0.07 (0.01)	0.01	2
I49C	ACh	39200 (1593)	1828 (116)	2285 (145)	17.2 (0.42)	0.6	3
I49Y	ACh	39280 (4000)	3574 (316)	4468 (395)	8.8 (0.45)	0.3	3

All values pertain to fully liganded AChRs. k_o, apparent opening rate constant; k_c^{obs}, observed closing rate constant; k_c^{cor}, closing rate constant corrected for channel block; K_{eq}, diliganded gating equilibrium constant; normalized K_{eq} (divided by the wt value for the salient agonist); *n*, number of patches. The mutant/wt ratio is with regard to the diliganded gating equilibrium constant.

[a]From Mitra et al. (2005).

[b]From Chakrapani and Auerbach (2005).

side chains H, W, or F increased K_{eq} (F by ~59-fold). There was no correlation between side chain hydrophobicity or volume and the change in K_{eq}. The change in K_{eq} in AChRs having D vs. F at position 127 (in both α subunits) was ~290,000-fold, which represents an energy difference of ~7.4 kcal/mol. For comparison, the maximum fold-changes in K_{eq} caused by mutations of some other α-subunit residues are shown in Table II. In our hands, Y127 is the most sensitive position ever reported for a point side chain substitution in both α subunits. The substantial changes in K_{eq} indicate that the energetic consequences of the mutations are substantially different in C vs. O, which implies that αY127 changes its structure, environment, or both (i.e., moves) in the gating reaction.

The mutation-induced changes in K_{eq} at αY127 arose mainly from changes in the channel opening rate constant (k_o). Fig. 3 shows a REFER analysis (a log–log plot of k_o vs. K_{eq}) of the mutational series at αY127. Each ~10-fold change in K_{eq} arose, on average, from an ~6.2-fold change in k_o and an ~1.6-fold change in k_c. The slope of this relationship, Φ, was 0.77 ± 0.02. Notice that the results for AChRs activated by different agonists scatter about the same line and that the Φ estimate was similar regardless of whether the AChRs were activated by acetylcholine (0.85 ± 0.04), carbamylcholine (0.75 ± 0.2), or choline (0.75 ± 0.04) (Fig. 3).

The Φ-value for αY127 is the same as those for several residues in loop 2 and the cys-loop (Φ = 0.80 ± 0.05 and 0.78 ± 0.03) (Jha et al., 2007) and R209 in the pre-M1 linker (0.74 ± 0.02, on an E45A background) (Purohit and Auerbach, 2007), but is different from those for the transmitter binding site (0.93 ± 0.02) (Grosman et al., 2000) and residue αD97 in loop A (0.93 ± 0.03) (Chakrapani et al., 2003). This result suggests that position 127 moves relatively early in the diliganded channel-opening process and that its gating motions are correlated temporally with other residues in the second (Φ = 0.78) gating block, but that these occur after those in the first (Φ = 0.93) gating block.

TABLE II

The Changes in Gating Energy for some Extracellular Domain Residues in AChR

Constructs	Location	Fold-change	ΔΔG (kcal/mol)	Reference
Y93W	Loop A	129	2.9	Akk et al., 1999
D97A	Loop A	167	3.0	Chakrapani et al., 2003
V46E	Loop 2	208	3.1	Chakrapani et al., 2003
V46A	Loop 2	474	3.6	Lee and Sine, 2005
E45K	Loop 2	120	2.8	Lee and Sine, 2005
E45H	Loop 2	2,170	4.5	Purohit and Auerbach, 2007
S269I	M2–M3 linker	115	2.8	Mitra et al., 2005
I274T	M2–M3 linker	2,014	4.4	Jha et al., 2007
P272G	M2–M3 linker	159	3.0	Lee and Sine, 2005
V132F	Cys-loop	2,820	4.5	Jha et al., 2007
F135A	Cys-loop	3,125	4.7	Chakrapani et al., 2003
Q140A	Cys-loop	658	3.8	Chakrapani et al., 2003
D200N adult	β10-strand	368	3.5	Akk et al., 1996
D200N embryonic	β10-strand	1,283	4.2	Akk et al., 1996
R209Q	Pre-M1	46	2.3	Lee and Sine, 2005
εP121L	β6-β6' strand	290	3.3	Ohno et al., 1996
εD175N	β8-β9' strand	79	2.6	Akk et al., 1999
εE184D	β8-β9' strand	56	2.4	Akk et al., 1999

Fold-change in gating equilibrium constants are from the literature and for diliganded gating using single channel analysis. $\Delta\Delta G = -RT \ln(K_{eq}^{wt}/K_{eq}^{mut})$.

We measured the single-site association and dissociation rate constants (k_+ and k_-) and equilibrium dissociation constant ($k_+/k_- = K_d$) for ACh binding to the closed conformation in one mutant construct, Y127C (Fig. 4). In this mutant K_d = 144 μM, which is in the range of previous measurements for wild-type AChRs exposed to 140 mM NaCl (100–150 μM) (Akk and Auerbach, 1996; Chakrapani et al., 2003). Similarly, the association and dissociation rate constants in the mutant, $k_+ = 2.10^8\ M^{-1}s^{-1}$ and $k_- = 3.0 \times 10^4\ s^{-1}$, were similar to wt values.

We also probed the effects on gating of mutations to residues in the β, ε, and δ subunits that are homologous to αY127. In the non–α subunits, which are homologous in both sequence and structure to the α subunits in the vicinity of αY127, the residue in question (βS127, εT127, or δS129) immediately preceded in sequence the extracellular disulfide bond. Seven mutations of these three positions all yielded AChRs having wt-like gating behaviors (Table IV).

αI49, δI43, and εN39

We next examined the gating properties of AChRs having mutations of residues that are close to αY127 (Fig. 1 B). αI49 is at the N terminus of β-strand 2, ∼5 Å from αY127. The gating kinetics for three mutants of this position, C, V, and Y, did not change K_{eq} by greater than threefold (Table I). Thus, we have no evidence that the αI49 side chain moves relative to its local environment between C and O conformations.

εN39 or δI43 are neighbors of αY127 in the companion, non–α subunit. A REFER analysis of position δI43 is shown in Fig. 5. All four of the tested substitutions decreased K_{eq}, with $\Phi = 0.86 \pm 0.10$. Although this result indicates that δI43 moves early in the reaction, we are unable to distinguish this Φ-value from those of the first (0.93; agonist and loops A, B, and C) and second (0.77; Y127, loop 2, and cys-loop) blocks of the α-subunit. At εN39, F and D substitutions caused a small (less than threefold) change in K_{eq}, and the substitution of an Ile at this position also generated currents having wt-like kinetic behavior (when activated by 30 μM ACh). The substitution of an H increased the cluster open probability relative to the wt, but the kinetics of these intracluster intervals was complex, with at least two conducting and two nonconducting states apparent. Therefore, unambiguous values of k_o and k_c could not be estimated. These results suggest that εN39 moves during gating, but we were unable to estimate a Φ-value for this position.

Coupling of αY127 Gating Motions within and between Subunits

In the α-subunit, two residues in loop A, part of which contributes to the transmitter binding site, may be close to αY127: αD97 and αN94. Mutation of αD97 causes a substantial change in K_{eq} and has a Φ-value that is different from that of αY127 (0.93 vs. 0.77). We therefore tested whether an interaction between αY127 and αD97 couples the gating motions (energy transfer) between the transmitter binding site (in the first Φ-block) and the cys-loop (in the second Φ-block).

We probed a D97↔Y127 interaction by measuring the gating kinetics of AChRs having a mutation (in both

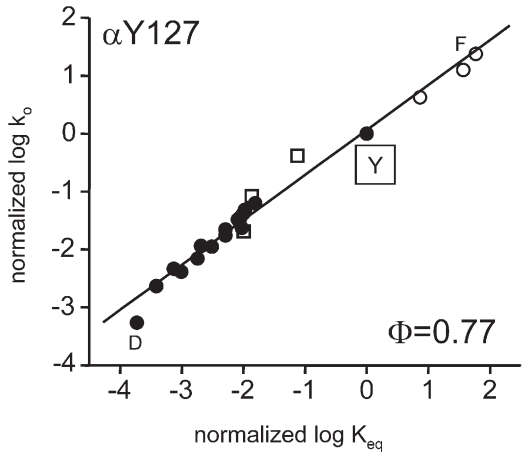

Figure 3. REFER analyses for αY127. Each point represents the mean of greater than two patches (Table I). Φ-Value was estimated as the slope of an unweighted linear fit to a log–log plot of normalized k_o vs. normalized K_{eq} for all 19 mutants. The slope Φ = 0.77 ± 0.02 makes αY127 a member of the second Φ-block that includes the cys-loop and loop 2. The open circles, filled circles, and open squares are choline, ACh, and carbamylcholine data points, respectively.

α subunits) at both of these positions (Table III). Six pairwise combinations were tested, with two different side chains at Y127 (H and C) and three different side chains at D97 (M, Y, and H). By themselves, the mutations at position 127 either reduced K_{eq} (C, by 201-fold) or increased K_{eq} (H, by 7.3-fold), while those at position 97 always increased K_{eq} (M, Y, or H, by 5.5-, 20-, and 7.3-fold, respectively). The hallmark of energetic coupling between αY127 and αD97 is a fold-change in K_{eq} with both sites mutated that is not equal to the product of the fold-changes for each site mutated.

With Y127H (activated by choline), the observed values of K_{eq} for the three D97 mutants were, on average, modestly (∼2.5-fold) smaller than predicted assuming independence (Table III). With the Y127C constructs (activated by ACh), the observed values of K_{eq} for the three D97 mutants were close to those predicted assuming independence. The average coupling energy was 0.53 kcal/mol for the Y127H background and −0.37 kcal/mol for the Y127C background. These results suggest that the magnitude of the coupling energy can vary with the side chain substitution. However, the coupling energy was small for both of the two tested backgrounds, especially when one considers that this coupling energy is spread between two Y127–D97 pairs (two α subunits). Overall, the results suggest that although a large magnitude of energy change is associated with positions D97 and Y127 when examined individually, a D97↔Y127 perturbation in combination is not an important component of energy transfer within the transition state of diliganded gating. The assumption that the residues may be interacting at the Φ-block boundaries, however, is based on the proximity of the two residues in the *Torpedo* AChR structure. Two problems with this assumption are that Y127 and D97 are >9 Å apart in the mouse α-subunit fragment structure, and that neither structure reflects a ligand-bound AChR. There is a reason to suspect that

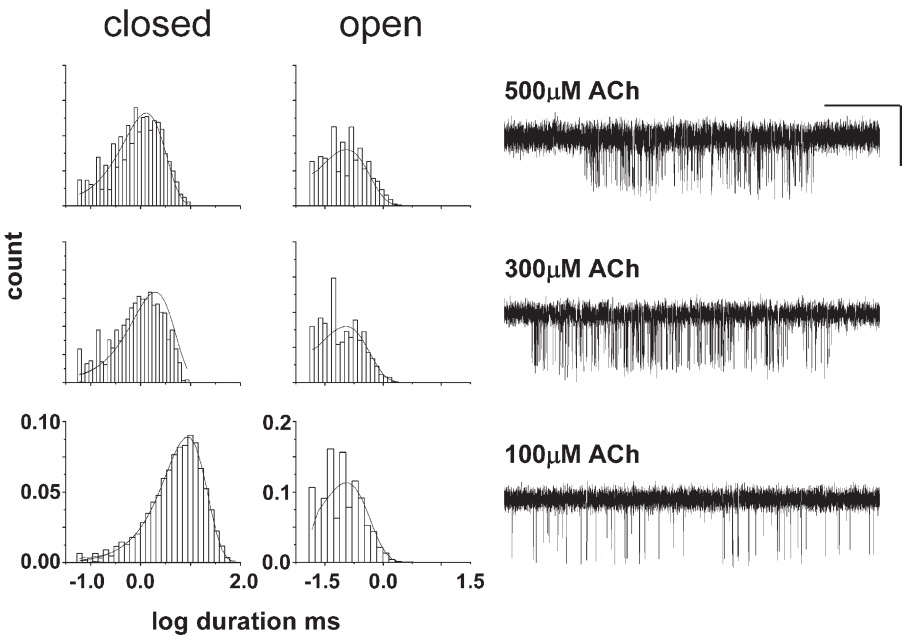

Figure 4. The mutation αY127C does not alter the closed-channel equilibrium dissociation constant. Left, open and closed interval duration histograms at different ACh concentrations. The solid lines are calculated from the globally optimized rate constants. Number of events analyzed at various concentrations of ACh were: 100 μM, 3391; 300 μM, 2244; and 500 μM, 6940. Right, example clusters from each concentration. The optimal rate constants were: k_+ (single-site association) = 205 μM s^{-1}, k_- (single-site dissociation) = 29604 s^{-1}, k_o = 2089 s^{-1}, and k_c = 5032 s^{-1}. We calculate K_d (=k_-/k_+) = 144 μM for the mutant. For comparison, the wt estimates are k_+ = 167 μM s^{-1} and k_- = 24,745 s^{-1}, K_D = 148 μM (Chakrapani and Auerbach, 2005). There is no significant effect of this mutation on ACh binding to closed AChRs and we speculate that αY127 mutations that change K_{eq} do so by changing the unliganded gating equilibrium constant rather than the closed/open affinity ratio. Calibration bars for single channel traces: (horizontal scale bar = 100 ms, vertical scale bar = 6 pA).

TABLE III

Kinetic and Coupling Analyses for αY127 and αD97, δI43, and εN39 Mutants

Construct	Agonist	k_0 (s^{-1})	k_c^{obs} (s^{-1})	k_c^{cor} (s^{-1})	K_{eq} (k_o/k_c^{cor})	Normalized K_{eq} (mut/wt) Observed	Predicted	ΔΔG	*n*
wt	Cho	120	–	2583	0.046	1.0	–	–	
wt	ACh	48000	–	1700	28.2	1.0	–	–	
D97H	Cho	1364 (19)	480	1282 (80)	1.06 (0.05)	23	–	–	2
D97Y	Cho	1420 (29)	563	1503 (48)	0.95 (0.03)	20.5	–	–	3
D97M	Cho	462	680	1816	0.25	5.5	–	–	1
Y127H	Cho	520 (68)	577 (86)	1541 (295)	0.33 (0.01)	7.3	–	–	4
Y127C	ACh	862 (119)	4674 (248)	5843 (310)	0.14 (0.03)	0.005	–	–	4
Y127H+D97H	Cho	5066 (166)	649 (66)	1734 (176)	2.98 (0.3)	65	167.9	0.55	3
Y127H+D97Y	Cho	6033 (540)	904 (19)	2414 (52)	2.5 (0.3)	54	150	0.61	3
Y127H+D97M	Cho	3338 (228)	1437 (234)	3837 (624)	0.93 (0.19)	18.9	40.2	0.44	3
Y127C+D97H	ACh	13400 (1249)	2694 (181)	3368 (226)	4.00 (0.64)	0.14	0.04	−0.80	2
Y127C+D97Y	ACh	16230 (204)	4601 (111)	5751 (139)	2.82 (0.03)	0.1	0.1	0.01	2
Y127C+D97M	ACh	6085 (924)	3503 (176)	4379 (220)	1.39 (0.18)	0.05	0.03	−0.34	3
δI43N	ACh	5395	1472	1840	2.93	0.1	–	–	1
δI43H	ACh	3820 (227)	1546 (159)	1932 (198)	2.04 (0.31)	0.07	–	–	3
δI43T	ACh	4778 (278)	2768 (160)	3460 (200)	1.4 (0.16)	0.05	–	–	3
δI43A	ACh	2424 (266)	1948 (458)	2434 (572)	1.1 (0.36)	0.04	–	–	2
αY127H+δI43H	Cho	530 (33)	1980 (38)	5285 (100)	0.1 (0.004)	2.16	0.5	0.84	2
εN39F	ACh	27776	2210	2763	10.1	0.4	–	–	1
εN39D	Cho	40 (2)	882 (87)	2354 (231)	0.017 (0.001)	0.4	–	–	3
εN39H	Cho	ND	ND	ND	ND	ND	ND	ND	–
εN39I	ACh	ND	ND	ND	ND	ND	ND	ND	–

Mutations of αD97 (M, H, and Y) on Y127H or Y127C constructs generally showed a fold-change in K_{eq} approximately half that predicted from the product of the single-mutant fold-change. The coupling energies for both double mutant series are small, suggesting that the coupling energy is distributed across multiple sites along between the first and second Φ blocks.

loop A moves as a consequence of agonist binding (in addition to channel gating), so we do not know the separation between these residues in fully liganded AChRs.

We next measured the extent of coupling between αY127H (7.3-fold increase in K_{eq}) and δI43H (13.8-fold decrease). Together, these mutations caused a 2.2-fold increase in K_{eq}, whereas if they were independent we would expect a 1.9-fold decrease in K_{eq}. This approximately fourfold effect indicates that there is modest degree of coupling between the αY127 and δI43 side chains (+0.84 kcal/mol; Table IV). Note that this interaction occurs at a single subunit interface and should therefore be considered to be substantially greater than the αY127–αD97 interaction.

αK145

We measured the gating rate constants for four different mutations of αK145, which is on β-strand 6 (Fig. 1). In the unliganded *Torpedo* structure, this residue is within 4 Å αD200 and loop A residue αY93, two residues that have been shown to move during diliganded C-O gating. K145 is also likely to be close to moving-residue αY190 (Chen et al., 1995) when the transmitter binding site is occupied by an agonist (Celie et al., 2004). Finally, αK145 is near αT202, a residue that has not yet been probed at the rate constant level.

All four of the mutations of K145 (C, A, R, and D) decreased K_{eq}, by up to 282-fold (Table V). The causes of these decreases were, in all cases, almost exclusively due to decreases in k_o. Fig. 6 shows the REFER for αK145. The Φ-value was 0.96 ± 0.04.

DISCUSSION

Comparison with Previous Results

Mukhtasimova and Sine (2007) studied the kinetic behavior of two αY127 mutants (F and T) plus εN39A and δN41A. Further, they measured the coupling between three pairs and two triplet combinations of these mutants. Although they studied human AChRs activated by ACh in 142 mM KCl and we studied mouse AChRs activated by ACh or choline in 140 mM NaCl, both sets of results are in general agreement. Mutations to Y127 have a profound effect on channel gating (K_{eq}), and this residue is a site where gating motions are coupled between subunits.

The main difference in the two sets of results is in relation to the αY127F mutation. We measured a much larger increase in K_{eq} for Y127F (58.7-fold vs. 2.2-fold increase). We speculate that this difference can be traced to an immeasurably fast opening rate constant for this construct in the experiments where the mutant AChRs were activated by ACh. In wt AChRs the difference in

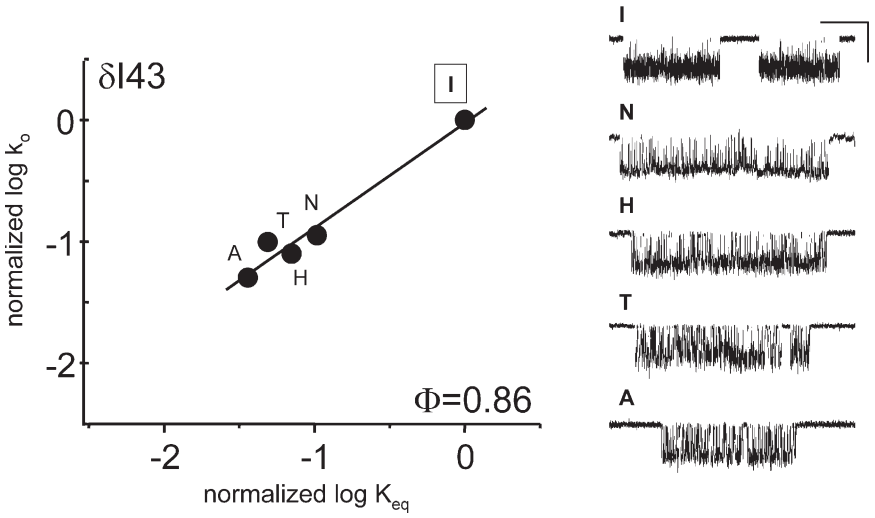

Figure 5. REFER analyses for δI43. Each point represents the mean of greater than two patches (Table IV). Φ-Value was estimated as the slope of an unweighted linear fit to a log–log plot of normalized k_o vs. normalized K_{eq} for all four mutants. The slope, Φ = 0.86 ± 0.10. Calibration bars for single channel traces: horizontal scale bar = 100 ms, vertical scale bar = 6 pA.

K_{eq} for different agonists is manifest almost exclusively as a difference in the opening rate constant (Φ = 0.93; Grosman et al., 2000). Assuming that this pattern pertains to the Y127F mutant, then k_o with ACh should be ∼400 times larger than k_o with choline (Chakrapani and Auerbach, 2005). In this case, our measurement for k_o with choline (2853 s^{-1}) translates to an opening rate of k_o with ACh of $>10^6$ s^{-1}, which is too fast to be detected experimentally. Perhaps the brief gaps observed in the experiments with human AChRs (Fig. 2 and Table II in MS) did not arise from C↔O gating but rather from channel block by the agonist or some other process. Our results do not agree with the proposal that aromatic side chains can be substituted at position αY127 without consequence.

Mukhtasimova et al. (2005) also measured the gating rate constants for E, Q, and A mutants of αK145. They report that these mutations decrease k_o but leave k_c essentially unchanged is consistent with our estimated Φ value of 0.96 for this position.

Structure–Function

A D-to-F side chain substitution at αY127 changes K_{eq} by nearly ∼290,000-fold. The magnitude of this change is substantially greater than that caused by any other ECD side chain substitution observed so far, even considering the fact that both α subunits carried the mutation. (The change in K_{eq} would be ∼540-fold if the energy difference between C and O was equally distributed between the two α subunits).

The relationship between a change in structure and the magnitude of the change in K_{eq} is complex. Although we measured K_{eq} for all 20 natural side chains at αY127 and for four side chains at αK145, we are nonetheless unable to draw strong conclusions about the chemical natures of the forces behind the αY127 gating motions. We note, however, that the mutations of αY127 that increased K_{eq} are aromatic and flat. There is no apparent correlation between side chain volume or hydrophobicity and the magnitude of the change in K_{eq}. Also, the charged side chains D, K, R, and E all reduced K_{eq} at αY127 (by 4847-, 1282-, 553-, and 104-fold, respectively), and D and R reduced K_{eq} at αK145 (by 282- and 60-fold, respectively), so the sign of the charge at both of these positions appears not to be an important determinant of K_{eq}.

The gating motion of αK145 (as evidenced by the mutation-induced change in K_{eq}) occurs approximately synchronously (same Φ-value) as other residues near the

TABLE IV

Kinetic Analyses of α127 Homologous Residues in Non–α Subunits

Construct	Agonist	k_0 (s^{-1})	k_c^{obs} (s^{-1})	k_c^{cor} (s^{-1})	K_{eq} (k_o/k_c^{cor})	Normalized K_{eq} (mut/wt)	*n*
βS127A	Cho	53	1296	3460.3	0.015	3.1	1
βS127V	Cho	108	1305	3484.3	0.030	1.5	1
βS127Y	Cho	70	850	2269.5	0.030	1.5	1
δS129Y	ACh	23253	1874	2342.5	9.92	0.35	1
εT127A	Cho	138	1484	3962.3	0.034	0.74	1
εT127V	Cho	52	420	1121.4	0.046	1.0	1
εT127Y	ACh	30370	2550	3187.5	9.52	0.34	1

In β, δ, or ε subunit, none of the mutants at residues homologous to Y127 show fold-change in Keq greater than threefold. These residues may not be moving during AChR gating. The abbreviations used here are the same as indicated earlier.

TABLE V

Kinetic Analyses of AChR Mutants

Construct	Agonist	k_0 (s^{-1})	k_c^{obs} (s^{-1})	k_c^{cor} (s^{-1})	K_{eq} (k_o/k_c^{cor})	Normalized K_{eq} (mut/wt)	*n*
K145C	ACh	2030 (50)	1200 (126)	1500 (157)	1.38 (0.14)	0.05	3
K145A	ACh	1111 (102)	1385 (126)	1732 (157)	0.65 (0.08)	0.02	3
K145R	ACh	1061 (13)	1808 (85)	2260 (106)	0.47 (0.02)	0.016	3
K145D	ACh	210 (42)	1603 (4)	2003 (002)	0.10 (0.02)	0.004	2

All the mutants tested at position K145 produced loss of function constructs. The abbreviations used here are the same as indicated earlier.

transmitter binding site, in loops A, B, and C. The movement of αK145 is correlated temporally with the movement of its close neighbors αD200 and αY93. The movement of αY127 occurs after the movement of αK145, and approximately synchronously with residues in the cys-loop and loop 2.

Rotation Hypothesis

The mutation-induced changes in K_{eq} at positions αK145 and αY127 are consistent with the proposal that gating entails a rotation of the α-subunit β-sandwich core (Unwin et al., 2002). However, some observations of AChR function appear to be inconsistent with this hypothesis. (a) A substituted cysteine accessibility study of residues between L36 and I53 in strands β1 and β2 in the α7 AChR showed that the rates of reaction with MTSEA in the presence of ACh varied significantly (McLaughlin et al., 2007). However, the rate of reaction decreased and increased, respectively, for the closely apposed residues M40 and N52, a result that is unexpected for a rigid body rotation of the β-core. (b) The effects of mutations on K_{eq} have been measured for seven different residues that are in the inner β strands of the ECD core: αL40A (in strand 1), αI49C, V, and Y, αV54L, αR55A and W (in strand 2), and αA122L, αS126V and A, and αY127 (in strand 6). Of these constructs, only the αY127 mutants changed K_{eq} by greater than threefold and, hence, gave a clear indication of motion. Although the lack of change in K_{eq} does not unequivocally indicate a lack of gating motion, it would be surprising if a rotation altered the energetic environment only around αY127. More residues (Celie et al., 2004) and mutations in both the inner and outer leaflets of the β-core need to be tested to test the energetic consequences of such a rotation. (c) The asynchrony of motion (different Φ values) for αY127 and αK145 is unexpected if the β-core rotation was that of a rigid body motion. In summary, the results suggest that the hypothesis of a β-sandwich core rotation in the gating reaction is, at best, incomplete. Because the rotation hypothesis arose from a comparison of the structures of α vs. non–α subunits in unliganded AChRs, we speculate that such movements may occur upon ligand binding rather than channel gating.

Φ Map

Fig. 7 shows the map of Φ superimposed on the mouse α-subunit fragment structure (2qc1.pdb, Dellisanti et al., 2007). The Φ values for the purple residues are ∼0.93, those for the orange residues are ∼0.77, and the white residues show no indication of a gating motion (ΔK_{eq} < threefold). This pattern suggests that the diliganded gating motions in the α-subunit mainly propagate along the α-ε (α-δ) subunit interface.

Φ changes significantly (by ∼0.16 units) between αD97 and αY127 (which are within 4 Å in 2bg9.pdb and 9 Å in 2qc1.pdb), whereas Φ is the same for residues that

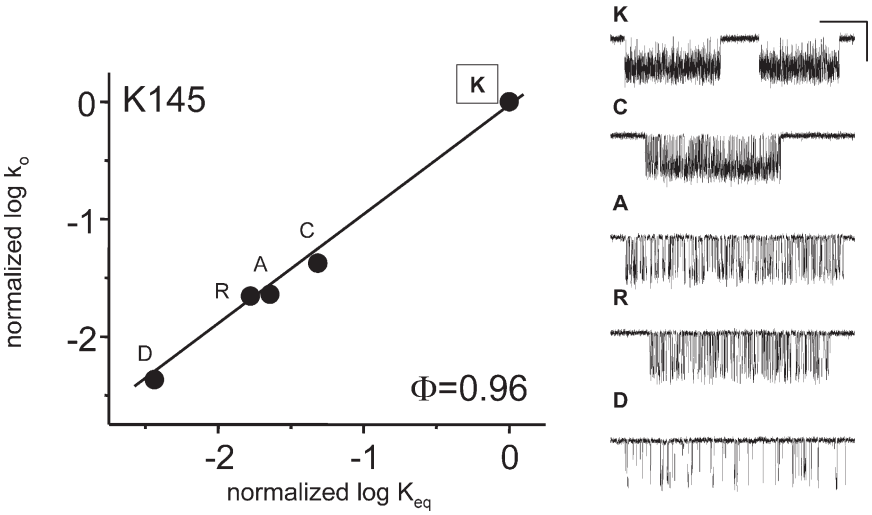

Figure 6. REFER analyses for αK145. Each point represents the mean of greater than two patches (Table V). The Φ-value estimated for K145 is Φ = 0.96 ± 0.04. Calibration bars for single channel traces: horizontal scale bar = 100 ms, vertical scale bar = 6 pA.

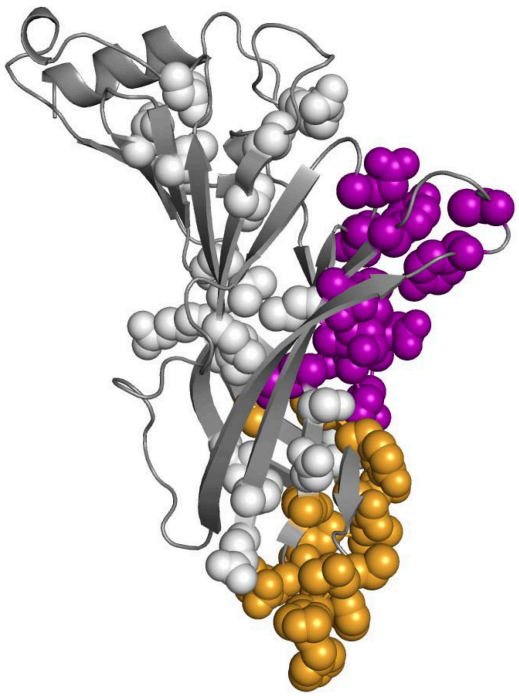

Figure 7. Gating movements occur mainly along the $\alpha/\varepsilon(\delta)$ subunit interface. The structure is the mouse α-subunit ECD fragment (2qc1.pdb). The diliganded gating rate constants have been measured for the residues shown as spheres. White: mutations resulted in little or no change in K_{eq} (less than threefold), hence these residues show no indication of undergoing a gating motion (positions 20, 29, 31, 35, 40, 49, 54, 55, 56, 65, 110, 116, 120, 141, 143, 146, 207, and 208). Colored: mutations significantly changed K_{eq}. Purple, $\Phi \approx 0.93$ (positions 93, 95–100, 144, 145, 149, 152, 153, 190, 192, 198, and 200). Orange, $\Phi \approx 0.77$ (positions 45–48, 127, 132, 133, 134, 135, 137, 138, 140, and 209). The channel opening gating motions in the α-subunit ECD appear to propagate mainly along the interface with the ε (or δ) subunit, with residues near the binding site moving before those near the ECD–TMD interface.

are separated by much larger distances. For example, residues separated by >20 Å and that have similar Φ values are αY127 and αF135 ($\Phi \sim 0.78$) and αD97 and αD152 ($\Phi \sim 0.93$). These results, along with similar comparisons elsewhere in the AChR, suggest that residues are grouped into contiguous domains within which members all have approximately the same Φ-value, and that Φ can change abruptly in space as expected from discrete boundaries. However, it is important to mention again that we cannot be certain that αD97 and αY127 are as closely apposed in the state of our reaction (the agonist-bound closed↔open) as they are in the unliganded *Torpedo* structure or the toxin-bound α-subunit fragment. The results indicate that first gating Φ-block extends at least to αK145, and perhaps to αM144, which has a Φ-value of 0.84 ± 0.05 (Chakrapani et al., 2004).

Coupling

Our results indicate that there is only a small amount of energetic coupling (<0.6 kcal/mol) between αY127 and αD97 even though these side chains are close, are mutation-sensitive, and have different Φ values (Fig. 1). It is therefore unlikely that an interaction between these two residues is an important link in the propagation of the AChR gating conformational wave.

Mukhtasimova and Sine (2007) found large coupling coefficients between the intersubunit pairs αY127T/εN39A (1.7 kcal/mol) and αY127T/δN41A (3.8 kcal/mol). Our estimate of coupling for the αY127H/δI43H pair was somewhat smaller (0.84 kcal/mol) but still larger than for the αY127/αD97 pair. Our results support the idea that αY127 is a site where the gating conformational cascade in the α- subunit is linked to that in the δ or ε subunits. The Φ- value of δI43 (0.86 ± 0.10) cannot be distinguished from those of either αD97 (0.93 ± 0.01) or αY127 (0.77 ± 0.02). Thus, we are unable to use Φ-value analysis to determine if the δ-subunit motions are synchronous with those of α, or, if not, which subunit precedes the other.

The Framework for AChR Gating

The results presented here and in the two companion papers support the idea that the framework for understanding the mechanism of diliganded AChR gating is that it is "brownian conformational wave." All of the 29 newly probed positions have Φ values that are similar to those previously reported for other amino acids in the extracellular region of the AChR α-subunit, and with magnitudes as expected based on location. There is little doubt that in the AChR, the map of Φ is highly organized and that residues are clustered into Φ blocks. Whatever mechanisms are proposed for AChR gating, and whatever physical interpretation is applied to Φ (relative timing, fractional side chain structure, multiple pathways), these must account for this highly ordered map of Φ values that has been derived from an extensive array of experiments.

The results do not support the notion that there is a single, rate-limiting structural transition that is the intersection of the C and O conformational ensembles. If there is a rotation of the α-subunit β-core, it is unlikely to be as a rigid body because αK145 on the outer sheet and αY127 on the inner sheet belong to two different Φ blocks. Although R209 and E45 both move and make a substantial energy contribution to the TR, these energy changes apparently do not arise from the perturbation of a salt bridge between this pair. The movement of the M2–M3 linker is an important TR event, but a full, cis–trans isomerization of the P272 or G275 backbone is not necessary for efficient gating. Rotations, electrostatic forces, changes in backbone bond angles, and hydrophobic interaction may occur in various regions of the protein, but each of these structural transitions contributes only a fraction to the total energy to the TR barrier.

Rather than conceiving of the energy barrier separating C from O as the point intersection of two parabolas,

the experimental results suggest that this TR barrier is a broad, corrugated, flat plateau (Auerbach, 2005). The map and range of Φ values, the spatially distributed effects of mutations on K_{eq}, and the rather weak coupling energies that we have observed between specific pairs of moving residues all suggest that the barrier for diliganded gating arises from the motions of many different metastable intermediate structures that are separated, sequentially, by small energy barriers. This energy distribution is certainly not isotropic, because some moving residues make larger energy contributions than others.

Several important regions of the AChR have not yet been mapped for Φ, including most of M1, the upper half of M2, and some regions of the ECD in the α-subunit, and many regions of the non–α subunits. This map of the TR, along with high resolution structures of the diliganded C and O end state ensembles, should serve as a guide for understanding the details of the structural transitions that constitute AChR gating.

We would like thank Mary Merritt and Mary Teeling for technical assistance.

Olaf S. Andersen served as editor.

Submitted: 17 July 2007
Accepted: 8 November 2007

REFERENCES

Akk, G. 2001. Aromatics at the murine nicotinic receptor agonist binding site: mutational analysis of the αY93 and αW149 residues. *J. Physiol.* 535:729–740.

Akk, G., and A. Auerbach. 1996. Inorganic, monovalent cations compete with agonists for the transmitter binding site of nicotinic acetylcholine receptors. *Biophys. J.* 70:2652–2658.

Akk, G., S. Sine, and A. Auerbach. 1996. Binding sites contribute unequally to the gating of mouse nicotinic αD200N acetylcholine receptors. *J. Physiol.* 496:185–196.

Akk, G., M. Zhou, and A. Auerbach. 1999. A mutational analysis of the acetylcholine receptor channel transmitter binding site. *Biophys. J.* 76:207–218.

Auerbach, A. 2005. Gating of acetylcholine receptor channels: Brownian motion across a broad transition state. *Proc. Natl. Acad. Sci. USA.* 102:1408–1412.

Auerbach, A. 2007. How to turn the reaction coordinate into time. *J. Gen. Physiol.* 130:543–546.

Brejc, K. 2001. Crystal structure of an ACh-binding protein reveals the ligand-binding domain of nicotinic receptors. *Nature.* 411:269–276.

Celie, P.H., S.E. van Rossum-Fikkert, W.J. van Dijk, K. Brejc, A.B. Smit, and T.K. Sixma. 2004. Nicotine and carbamylcholine binding to nicotinic acetylcholine = as studied in AChBP crystal structures. *Neuron.* 41:907–914.

Chakrapani, S., and A. Auerbach. 2005. A speed limit for conformational change of an allosteric membrane protein. *Proc. Natl. Acad. Sci. USA.* 102:87–92.

Chakrapani, S., T.D. Bailey, and A. Auerbach. 2003. The role of loop 5 in acetylcholine receptor channel gating. *J. Gen. Physiol.* 122:521–539.

Chakrapani, S., T.D. Bailey, and A. Auerbach. 2004. Gating dynamics of the acetylcholine receptor extracellular domain. *J. Gen. Physiol.* 123:341–356.

Chen, J., Y. Zhang, G. Akk, S. Sine, and A. Auerbach. 1995. Activation kinetics of recombinant mouse nicotinic acetylcholine receptors: mutations of α-subunit tyrosine 190 affect both binding and gating. *Biophys. J.* 69:849–859.

Corringer, P.-J., N.L. Novere, and J.-P. Changeux. 2000. Nicotinic receptors at the amino acid level. *Annu. Rev. Pharmacol. Toxicol.* 40:431–458.

Dellisanti, C.D., Y. Yao, J.C. Stroud, Z.Z. Wang, and L. Chen. 2007. Crystal structure of the extracellular domain of nAChR α1 bound to α-bungarotoxin at 1.94 Å resolution. *Nat. Neurosci.* 10:953–962.

Grosman, C., M. Zhou, and A. Auerbach. 2000. Mapping the conformational wave of acetylcholine receptor channel gating. *Nature.* 403:773–776.

Hansen, S.B., G. Sulzenbacher, T. Huxford, P. Marchot, P. Taylor, and Y. Bourne. 2005. Structures of *Aplysia* AChBP complexes with nicotinic agonists and antagonists reveal distinctive binding interfaces and conformations. *EMBO J.* 24:3635–3646.

Jha, A., D. Cadugan, P. Purohit, and A. Auerbach. 2007. Acetylcholine receptor channel gating at extracellular transmembrane domain interface: the cys-loop and M2–M3 linker. *J. Gen. Physiol.* 130:547–558.

Lee, W.Y., and S.M. Sine. 2005. Principal pathway coupling agonist binding to channel gating in nicotinic receptors. *Nature.* 438:243–247.

McLaughlin, J.T., J. Fu, and R.L. Rosenberg. 2007. Agonist-driven conformational changes in the inner β-sheet of α7 nicotinic receptors. *Mol. Pharmacol.* 71:1312–1318.

Mitra, A., G.D. Cymes, and A. Auerbach. 2005. Dynamics of the acetylcholine receptor pore at the gating transition state. *Proc. Natl. Acad. Sci. USA.* 102:15069–15074.

Mukhtasimova, N., C. Free, and S.M. Sine. 2005. Initial coupling of binding to gating mediated by conserved residues in the muscle nicotinic receptor. *J. Gen. Physiol.* 126:23–39.

Mukhtasimova, N., and S.M. Sine. 2007. An intersubunit trigger of channel gating in the muscle nicotinic receptor. *J. Neurosci.* 27:4110–4119.

Ohno, K., H.-L. Wang, M. Milone, N. Bren, J.M. Brengman, S. Nakano, P. Quiram, J.N. Pruitt, S.M. Sine, and A.G. Engel. 1996. Congenital myasthenic syndrome caused by decreased agonist binding affinity due to a mutation in the acetylcholine receptor [var epsilon] subunit. *Neuron.* 17:157–170.

Purohit, P., and A. Auerbach. 2007. Acetylcholine receptor gating at extracellular-transmembrane domain interface: the "pre-M1" linker. *J. Gen. Physiol.* 130:559–568.

Qin, F., A. Auerbach, and F. Sachs. 1997. Maximum likelihood estimation of aggregated Markov processes. *Proc. Biol. Sci.* 264:375–383.

Unwin, N. 2005. Refined structure of the nicotinic acetylcholine receptor at 4 Å resolution. *J. Mol. Biol.* 346:967–989.

Unwin, N., A. Miyazawa, J. Li, and Y. Fujiyoshi. 2002. Activation of the nicotinic acetylcholine receptor involves a switch in conformation of the α subunits. *J. Mol. Biol.* 319:1165–1176.